$LaBr_3$:Ce and silicon photomultipliers: Towards the optimal scintillating photon-counting detector

Stefan J. van der Sar*[a], David Leibold[a], Stefan E. Brunner[b], Dennis R. Schaart[a,c]
[a]Dept. of Radiation Science and Technology, Delft University of Technology, Mekelweg 15, 2629 JB, Delft, the Netherlands; [b]Broadcom Inc., Wernerwerkstrasse 2, 93049, Regensburg, Bavaria, Germany; [c]Holland Proton Therapy Center; Huismansingel 4, 2629 JH, Delft, the Netherlands.

ABSTRACT

We investigate fast silicon photomultiplier (SiPM)-based scintillation detectors for X-ray photon-counting applications, e.g., photon-counting computed tomography (CT). Such detectors may be an alternative to CdTe/CdZnTe (CZT) and Si detectors, which face challenges related to availability and cost-effective growth of detector-grade material, and detection efficiency, respectively. Here, we experimentally study energy response and count rate performance of a 1 mm × 1 mm single-pixel detector consisting of the readily available $LaBr_3$:Ce scintillator and an ultrafast SiPM.

We used three radio-isotopes and an X-ray tube for the experiments. Raw detector signals were processed by a second-order low-pass filter with a cut-off frequency f_c equal to 25 MHz or 100 MHz.

The detector pulse height was shown to be proportional to photon energy. We measured FWHM energy resolutions of 19.5% (f_c=25 MHz) and 21.5% (f_c=100 MHz) at 60 keV. The measured X-ray tube spectra showed signs of the expected features of such spectra. The best count rate performance was achieved using f_c=100 MHz. In case of paralyzable-like counting and a 30 keV counting threshold, the maximum observed count rate (OCR) was 10.5 Mcps/pixel. For nonparalyzable-like counting and the same threshold, the OCR appeared to approach an asymptotic value greater than 20 Mcps/pixel. These numbers are close to those of CdTe/CZT detectors highly optimized for photon-counting CT.

In conclusion, we show promising spectral X-ray photon-counting performance of an $LaBr_3$:Ce scintillation detector with SiPM readout. Depending on the application-specific requirements, miniaturization of the pixel size may be necessary, for which we discuss potential dose-efficient implementations.

Keywords: Count rate performance, energy response, scintillator, silicon photomultiplier, X-ray photon-counting.

1. INTRODUCTION

Photon-counting detectors (PCDs) for X-ray imaging, e.g., for diagnostic computed tomography (CT), are heavily investigated.[1,2] A PCD counts X-ray photon-induced detector pulses and registers them in one of at least two energy bins. This enables energy-resolved X-ray imaging. However, the task at hand is formidable, because the incident photon fluence rate may exceed 10^8 photons/mm/s,[3] so pulse pile-up is likely to distort the measurement of counts and energies.

The main detector concept under consideration at the moment is based on the mechanism of direct conversion, i.e., each X-ray photon absorbed in a semiconductor is directly converted into a number of electron-hole (e-h) pairs. This number is proportional to the absorbed energy. Under the influence of an electric field, the e-h pairs are separated and guided towards (pixelated) electrodes on which they induce a current pulse. The pulse processing chain then outputs pulses of which the height is a measure of the energy of the X-ray photon. The semiconductors used in the existing prototype CT scanners are CdTe,[4] CdZnTe (CZT),[5] and Si.[6]

* e-mail: s.j.vandersar@tudelft.nl; phone: +31 15 278 3776

7th International Conference on Image Formation in X-Ray Computed Tomography,
edited by Joseph Webster Stayman, Proc. of SPIE Vol. 12304, 123040A
 · 0277-786X · doi: 10.1117/12.2646519

Although such a detector outputs short pulses and allows for pixel size miniaturization (both help to reduce pile-up), the availability and cost-effective synthesis of CdTe/CZT detectors with a sufficiently low density of charge trapping centers (necessary to guarantee stable and reliable performance over time) remain issues.[2,7] On the other hand, Si detectors face challenges related to low density (ρ = 2.3 g cm^{-3}) and atomic number (Z = 14). Thus, it is not clear what the best choice of detector is, leaving room for developing other detector concepts.

We are therefore investigating fast scintillation detectors with silicon photomultiplier (SiPM) readout for X-ray photon-counting applications. This detector concept relies on the mechanism of indirect conversion, i.e., an X-ray photon is first converted into a pulse of optical scintillation photons, which is then converted into a current pulse by an SiPM (see figure 1a). The light pulse incident on the SiPM as a function of time t_1 after the X-ray interaction may be described as $A_1\exp(-t_1/\tau_d)$, with amplitude A_1 depending on deposited energy and τ_d the scintillation decay time constant. In order to mitigate pile-up, shorter τ_d than those of CsI (1 µs) and GOS (2.5 µs), the scintillators used in energy-integrating detectors, are needed.[8]

Each scintillator pixel must be coupled to its own SiPM. This light sensor consists of a two-dimensional array of single-photon avalanche diodes (SPADs, see figure 1b). The absorption of a single optical photon in a SPAD creates an e-h pair that can trigger an avalanche multiplication process providing a gain in the order of 10^6. The time profile of the SPAD current pulse as a function of time t_2 after the detection of an optical photon may be described as $A_2\exp(-t_2/\tau_r)$, with amplitude A_2 and recharge time constant τ_r. Since the SPADs on an SiPM are connected in parallel, the time profile of an X-ray photon-induced pulse is essentially a convolution of $A_1\exp(-t_1/\tau_d)$ and $A_2\exp(-t_2/\tau_r)$ (see figure 2). The high internal gain assures that the signal due to a single X-ray photon exceeds the noise level of the electronics (difficult to accomplish using conventional photodiodes) and potentially allows for a pulse processing chain relying only on simple current-to-voltage conversion and pulse height discrimination.

Since this detector concept is based on transport of photons rather than charges and various scintillators with high ρ and Z are readily available, it may provide a solution for the aforementioned difficulties of direct conversion detectors.

Here, we experimentally investigate the count rate performance of an ultrafast SiPM-based scintillation detector irradiated by a 120 kVp X-ray beam. The scintillator used in this study is $LaBr_3$:Ce, a commercially available scintillator that we previously identified as having favorable properties for high-rate, energy-resolved X-ray photon-counting.[8] We also study the energy response of the detector and compare our results with data from CdTe- and CZT-based PCDs.

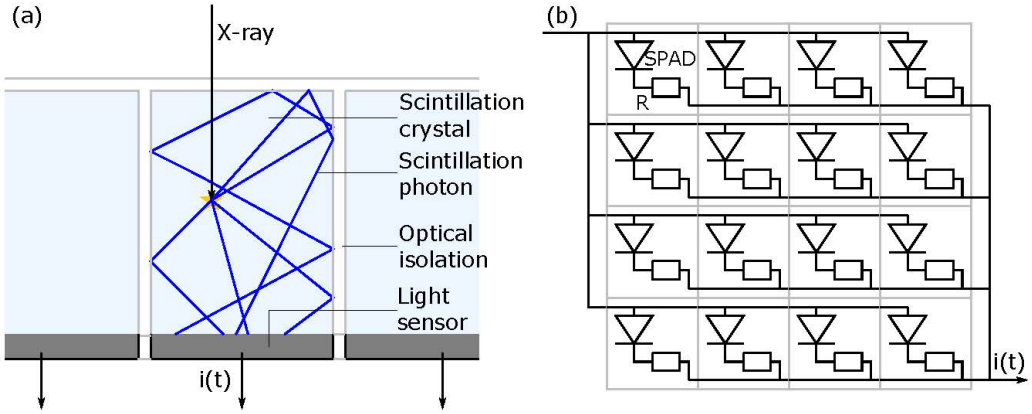

Figure 1. a) Schematic side view of a scintillation detector. Each pixel consists of a scintillation crystal, in which an X-ray photon is converted into a pulse of optical scintillation photons (~10^2 photons/keV), and each crystal is one-to-one coupled to a light sensor, which converts the light pulse into a current pulse $i(t)$. The isotropically emitted photons are guided towards the light sensor by a reflective optical isolation around the pixel, which also prevents light sharing among pixels (cf. charge sharing in semiconductor detectors). b) Schematic top view of a silicon photomultiplier (SiPM), which is the light sensor in our case. An SiPM is a two-dimensional array of single photon avalanche diodes (SPADs) connected in parallel. Typical SiPMs have ~10^2-10^4 SPADs per mm^2. When a SPAD detects an optical photon, an avalanche multiplication starts, which the resistor R quenches.[8]

2. MATERIALS AND METHODS

$LaBr_3$:Ce (5% Ce-doping, Saint Gobain Crystals) combines high X-ray detection efficiency (ρ=5.1 g cm^{-3}, Z_{La}=57, and Z_{Br}=35) with a short and intense scintillation pulse (τ_d=16 ns and a high light yield of 63 photons per keV). Using optically transparent glue, we coupled a 1 mm × 1 mm $LaBr_3$:Ce crystal to a 1.0 mm × 1.0 mm ultrafast SiPM (τ_r=7 ns, Broadcom Inc.). The $LaBr_3$:Ce crystal was 3.5 mm thick (equivalent to 2.5 mm CdTe in terms of detection efficiency in the diagnostic energy range). We also covered the crystal in reflective powder. Since $LaBr_3$:Ce is a hygroscopic scintillator, we applied an epoxy coating to our single-pixel detector, such that it can be used outside the moisture-free glovebox in which it was built. Note that the hygroscopic nature of a scintillator does not limit its applicability. The common NaI:Tl scintillator is also hygroscopic, and applied in detectors for clinical SPECT scanners, for example.

The current signals from the SiPM were converted into voltage signals by a trans-impedance amplifier (gain=10) before being digitized by a TeledyneLeCroy HDO9404 oscilloscope (sampling rate = 1 GHz, bandwidth = 200 MHz). Due to the finite number of optical photons per unit time in the scintillation pulse, the raw detector pulses are not perfect convolutions of $A_1\exp(-t_1/\tau_d)$ and $A_2\exp(-t_2/\tau_r)$, but show random fluctuations. In order to improve the accuracy of the measurement of counts and energies, all digitized signals were first smoothened by a second-order low-pass filter with a cut-off frequency f_c=25 MHz or f_c=100 MHz. The former should provide better low-rate energy resolution, the latter faster pulses (see figure 2a) and better counting performance.

In order to determine the (mean) pulse height as a function of energy, we recorded pulses while exposing the detector to three low-activity radioactive sources, one after another, with the following five photon emissions: 14 keV (Co-57), 32 keV (Ba-133), 60 keV (Am-241), 81 keV (Ba-133) and 122 keV (Co-57).

We conducted X-ray tube experiments using an Yxlon Y.TU 320-D03 tube, which had a tungsten target and an anode angle of 20°. A tube voltage of 120 kVp was selected and the beam was filtered by 3.0 mm Be and 7.5 mm Al in total. The resulting spectrum ranged from 20 keV to 120 keV. We then performed a tube current sweep starting at 0.5 mA and ending at 20 mA at fixed source-detector distance. For each tube current setting, we recorded ten pulse trains of 100 ms.

We determined the number of counts for thresholds at 15 keV and 30 keV, thereby covering a range of potential lowest-energy thresholds, which limit the count rate capability of PCDs. Additionally, we determined the number of counts for two counting algorithms. The first one is paralyzable-like (p-like) counting. Here, every positive threshold crossing leads to a count and the maximum signal before the subsequent negative threshold crossing is considered a measure of the energy. The second one is nonparalyzable-like (np-like) counting. In this case, we determine, after a fixed time period τ_{np} following the registration of a count, whether or not the signal from the detector is still above threshold. If yes, a second count will be registered, and so on. If not, the next count will only be registered when the next positive threshold crossing occurs. The maximum signal within the time period τ_{np} is considered a measure of the energy. The value of τ_{np} should exceed the time-over-threshold of the highest-energy pulses in order to prevent double counting of single pulses. We therefore used the pulses caused by the full absorption of 122 keV photons from the Co-57 source to determine proper values of τ_{np} for the detector (see figure 2b).

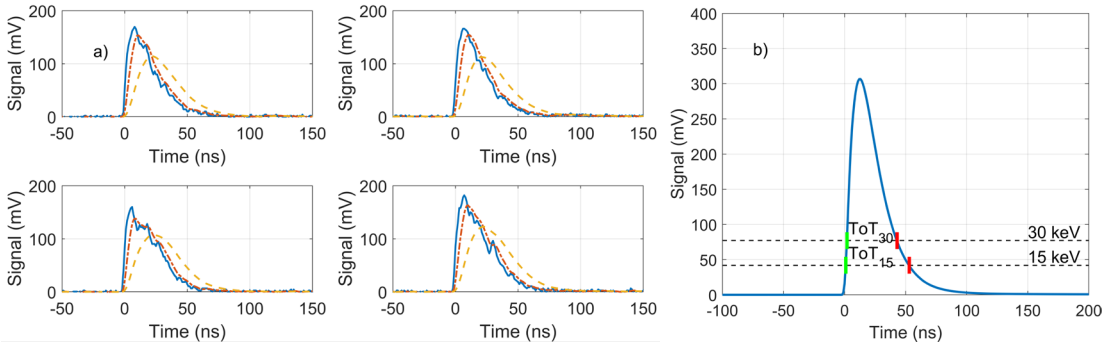

Figure 2. a) Four examples of pulses due to the full absorption of 60 keV photons. The solid curves are the raw pulses, and the dashed and dash-dotted curves describe these pulses after they have been smoothened by a second-order low-pass filter with a cut-off frequency f_c of 25 MHz and 100 MHz, respectively. b) Mean pulse shape for 122 keV photons and f_c=100 MHz. The start and end points of the time-over-threshold (ToT) at 15 keV and 30 keV used to determine τ_{np} are shown, too.

3. RESULTS AND DISCUSSION

Figure 3a and figure 3b show pulse height spectra obtained by exposing the detector to the Am-241 source and setting f_c to 25 MHz and 100 MHz, respectively. We observe the photopeak corresponding to the full absorption of 60 keV photons in the crystal. It is asymmetric due to overlap on its left hand side with a continuum of counts caused by photons that have first Compton scattered in the epoxy and/or powder around the crystal. We also notice a peak caused by a broad 11-22 keV X-ray emission from the source. It overlaps with a La K-escape peak at about 26 keV.

Both figure 3a and figure 3b also show that we fitted a 'single-sided' Gaussian to the photopeak in order to deal with aforementioned overlap. We then derived the mean pulse heights and the energy resolutions at 60 keV from the fits. Regarding the latter, we found 19.5% FWHM for f_c=25 MHz and 21.5% FWHM for f_c=100 MHz. 19.5% is comparable to what has been reported for at least one CdTe detector developed for photon-counting CT.[9] We used similar fits to determine the mean pulse heights corresponding to the four main peaks (energies) in the spectra of the other sources. The results are summarized in figure 3c and show that the detector has a proportional response in the relevant energy range.

By linear interpolation of the data points in figure 3c, we determined that the 15 keV and 30 keV thresholds for f_c=25 MHz are at 31.0 mV and 58.4 mV, respectively. In case f_c=100 MHz, these thresholds are at 41.8 mV and 77.2 mV.

Based on the mean shape of the pulses due to the full absorption of 122 keV photons from Co-57 (see figure 2b), the time-over-the x keV threshold for f_c=y MHz ($ToT_{x,y}$) was found to be: $ToT_{15,25}$=68 ns, $ToT_{30,25}$=55 ns, $ToT_{15,100}$=53 ns, and $ToT_{30,100}$=42 ns. Thus, we used these values of τ_{np}: $\tau_{np,15,25}$=70 ns, $\tau_{np,30,25}$=60 ns, $\tau_{np,15,100}$=55 ns, and $\tau_{np,30,100}$=45 ns.

Figure 4 shows the observed count rate (OCR) as a function of tube current I_{tube}. We estimated an incident count rate (ICR) for each value of I_{tube} by taking into account that ICR and I_{tube} are proportional to each other and by assuming that ICR=$OCR_{np,15,100}$ for I_{tube}=0.5 mA (the selected source-detector distance was such that the pile-up level was limited for I_{tube}=0.5 mA). The estimated ICRs are displayed on the top horizontal axes in figure 4 and indicate that we characterized the detector up to ICR≈31 Mcps/pixel. As expected, the curves for p-like counting feature a maximum OCR, which lies between 6 Mcps/pixel and 7.5 Mcps/pixel for f_c=25 MHz, and between 8 Mcps/pixel and 10.5 Mcps/pixel for f_c=100 MHz, depending on the threshold value. The curves for np-like counting should approach asymptotes defined by OCR=$1/\tau_{np}$ for high values of I_{tube}, i.e., they should approach OCRs of 14.3-16.7 Mcps/pixel for f_c=25 MHz and 18.2-22.2 Mcps/pixel for f_c=100 MHz, again depending on the threshold value. However, figure 4 shows that, especially for f_c=100 MHz, we did not reach these asymptotic values at the maximum available tube current of 20 mA yet. Thus, we plan to take measurements at shorter source-detector distances and to show the results at the conference.

To put the results into perspective, CdTe and CZT detectors that have been highly optimized for diagnostic photon-counting CT aim for a maximum OCR of 10-15 Mcps/pixel in case of p-like counting (e.g., the CZT detector in the prototype scanner of Philips[5]) or an OCR approaching 25-30 Mcps/pixel in case of np-like counting (e.g., the CdTe detector in the prototype scanner of Siemens[4]). The present results show that our prototype $LaBr_3$:Ce detector already approaches these numbers closely.

The rate capability per mm^2 can be improved by having multiple pixels on a square millimeter. However, the reflective isolation between pixels (see figure 1a) then starts to form a relatively large X-ray insensitive area that limits the achievable OCR and dose efficiency. However, Canon managed to manufacture an energy-integrating detector for its Aquilion Precision CT scanner that has scintillator pixels of such small dimensions with very thin reflective septa, such that the dose efficiency of conventional scanners is conserved. Even dead area-free options exist, such as a columnar microstructure of the scintillator (cf. the CsI scintillator in flat panel detectors),[10] and laser-induced optical barriers.[11]

Lastly, examples of X-ray tube spectra measured using the $LaBr_3$:Ce detector under low fluence rate conditions (i.e., I_{tube}=0.5 mA) are shown in figure 5. The typical shape of such spectra is clearly present in the data, including signs of the characteristic X-rays from the tungsten target of the tube. For photon energies exceeding 80 keV, the spectral intensity gradually decreases towards the maximum energy of 120 keV, with some overflow to higher energies because of the finite energy resolution of the detector and some pulse pile-up.

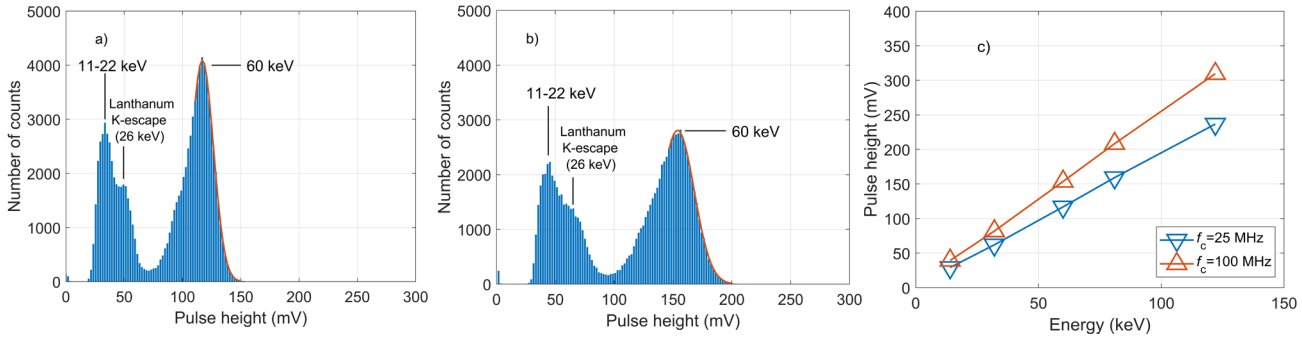

Figure 3. a) An Am-241 pulse height spectrum measured using the $LaBr_3$:Ce detector and a second order low-pass filter with cut-off frequency f_c=25 MHz. We fitted a 'single-sided' Gaussian to the 60 keV peak in order to determine the FWHM pulse height resolution, because the peak overlaps on the left with a continuum of counts caused by photons that have first Compton scattered in the epoxy and/or powder around the detector. b) The same Am-241 spectrum measured using the same detector, but a filter with f_c=100 MHz. c) Results of the pulse height calibration, showing highly proportional behavior.

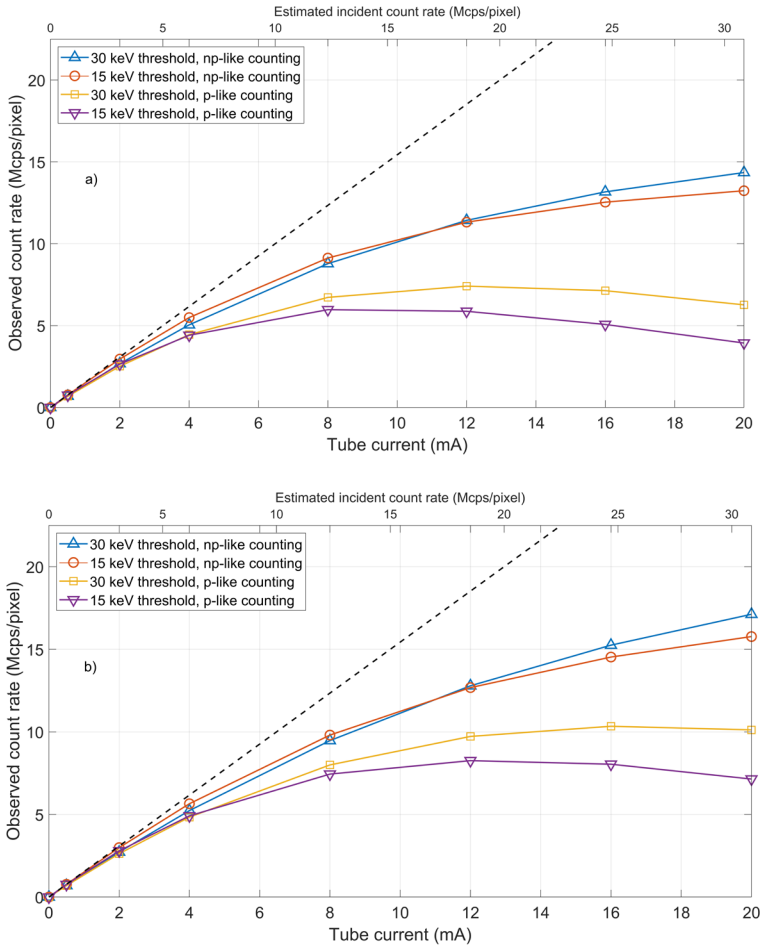

Figure 4. Observed count rate as a function of tube current, counting algorithm, and low-energy threshold for a) the $LaBr_3$:Ce detector and a second order low-pass filter with cut-off frequency f_c=25 MHz and b) the same detector, but a filter with f_c=100 MHz. The top horizontal axes display our estimates of the incident count rate corresponding to each value of the tube current. The dashed lines represent ideal counting, i.e., the observed count rate equaling the incident count rate.

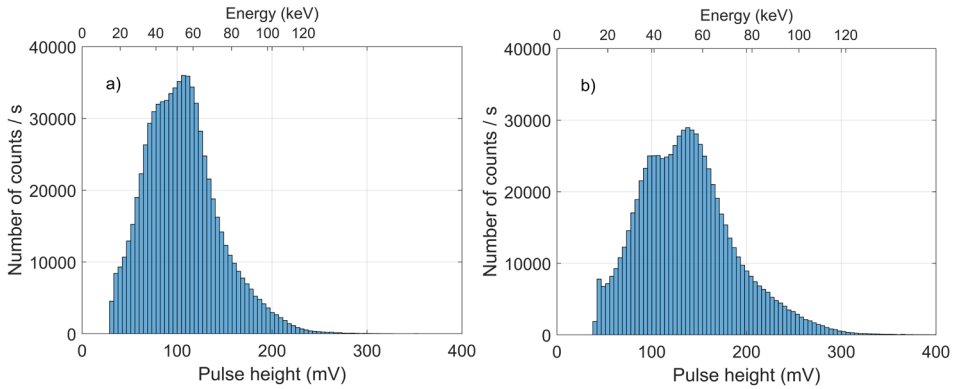

Figure 5. X-ray tube spectra (120 kVp, tungsten anode, anode angle of 20°, 3.0 mm Be and 7.5 mm Al filtration) measured using a) the $LaBr_3$:Ce detector and a second order low-pass filter with cut-off frequency f_c=25 MHz and b) the same detector, but a filter with f_c=100 MHz, for p-like counting and a 15 keV threshold under low fluence rate conditions (i.e., a tube current of 0.5 mA). The energy-axes are based on the pulse height calibrations shown in figure 3c.

4. CONCLUSIONS

We are investigating fast scintillation detectors with SiPM readout as alternatives to direct-conversion detectors for (clinical) X-ray photon-counting applications. In this work, we built a 1 mm × 1 mm single-pixel detector consisting of the fast and commercially available $LaBr_3$:Ce scintillator and an ultrafast SiPM. We measured energy resolutions around 20% FWHM at 60 keV, slightly depending on the cut-off frequency of the filter used in the pulse processing chain. Moreover, we were able to measure an X-ray tube spectrum with signs of its characteristic features. We also measured count rate curves and found a maximum observed count rate (OCR) of 10.5 Mcps/pixel for paralyzable-like counting, a threshold of 30 keV, and a cut-off frequency of 100 MHz. In case of nonparalyzable-like counting, the OCR seemed to approach an asymptotic value exceeding 20 Mcps/pixel. The results mean that the performance of our prototype detector already approaches that of CdTe and CZT detectors highly optimized for photon-counting CT.

REFERENCES

[1] S.S. Hsieh et al., "Photon counting CT: Clinical applications and future developments", IEEE Transactions on Radiation and Plasma Medical Sciences 5(4), 441-452 (2020). doi: 10.1109/TRPMS.2020.3020212.

[2] T. Flohr et al., "Photon-counting CT review", Physica Medica 79, 126-136 (2020). doi: 10.1016/j.ejmp.2020.10.030.

[3] M. Persson et al., "Upper limits of the photon fluence rate on CT detectors: Case study on a commercial scanner", Medical Physics 43(7), 4398-4411 (2016). doi: 10.1118/1.4954008.

[4] S. Kappler et al., "Photon counting CT at elevated tube currents: Contrast stability, image noise, and multi-energy performance", Proceedings of SPIE 90331C (2014). doi: 10.1117/12.2043511.

[5] R. Steadman et al., "ChromAIX2: A large area, high count-rate energy-resolving photon-counting ASIC for a …", Nuclear Instruments and Methods in Physics Research A 862, 18-24 (2017). doi: 10.1016/j.nima.2017.05.010.

[6] J. da Silva et al., "Resolution characterization of a silicon-based, photon-counting computed tomography prototype capable of patient scanning", Journal of Medical Imaging 6(4), 043502 (2019). doi: 10.1117/1.JMI.6.4.043502.

[7] U.N. Roy et al., "Role of selenium addition to the CdZnTe matrix for room-temperature radiation detector applications", Scientific Reports 9, 1620 (2019). doi: 10.1038/s41598-018-38188-w.

[8] S.J. van der Sar et al., "Silicon photomultiplier-based based scintillation detectors for photon-counting CT: A feasibility study", Medical Physics 48(10), 6324-6338 (2021). doi: 10.1002/mp.14886.

[9] R. Steadman et al., "ChromAIX: Fast photon-counting ASIC for spectral computed tomography", Nuclear Instruments and Methods in Physics Research A 648, S211-S215 (2011). doi: 10.1016/j.nima.2010.11.149.

[10] H.B. Bhandari et al., "Large-area crystalline microcolumnar $LaBr_3$:Ce for high-resolution gamma ray imaging", IEEE Transactions on Nuclear Science 60(1), 3-8 (2013). doi: 10.1109/TNS.2012.2213612.

[11] H. Sabet et al. "A sub-mm spatial resolution LYSO:Ce detector for small animal PET", IEEE Nuclear Science Symposium and Medical Imaging Conference (2015). doi: 10.1109/NSSMIC.2015.7582201.